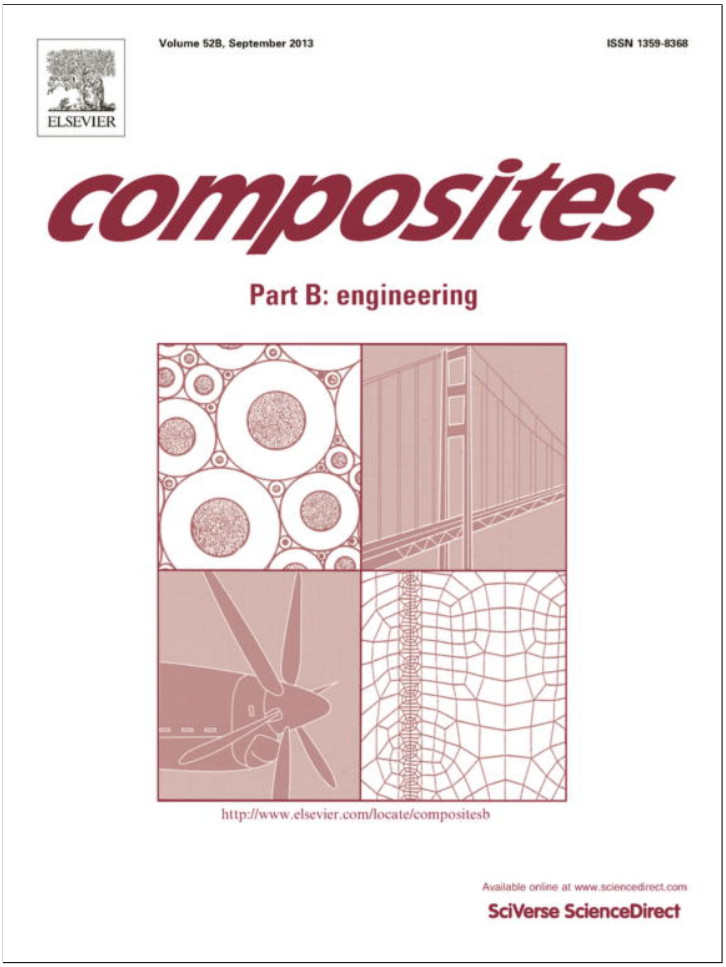

Composites: Part B 52 (2013) 187–198

Contents lists available at SciVerse ScienceDirect

Composites: Part B

journal homepage: www.elsevier.com/locate/compositesb

A layerwise/solid-element method of the linear static and free vibration analysis for the composite sandwich plates

Dinghe Li, Yan Liu, Xiong Zhang *

School of Aerospace, Tsinghua University, Beijing 100084, China

ARTICLE INFO

Article history:
Received 18 December 2012
Received in revised form 13 March 2013
Accepted 7 April 2013
Available online 18 April 2013

Keywords:
A. Laminates
B. Vibration
C. Finite element analysis (FEA)
Layerwise theory

ABSTRACT

In the traditional analysis schemes of the composite sandwich structures the core is firstly simplified as an equivalent anisotropic material and then modeled by the plates and shells theories. Its main disadvantage is that the equivalent core will result in large equivalent error especially in the key area and the thick core will further reduce the analysis accuracy of the plates and shells theories. Therefore, a layerwise/solid-element method (LW/SE) is proposed in this paper, in which the layerwise theory is used to model the behavior of the composite laminated facesheets while the eight-noded solid element is employed to discretize the core. Three models, the full model, the local model and the equivalent model, are presented to model the core. Several numerical examples are investigated and the static analysis and free vibration analysis of the composite sandwich plates are tested. The results of proposed method are in good agreement with those of 3D finite element model. A detailed comparative study is conducted to investigate the performance of three modeling schemes for static analysis and free vibration analysis problems.

1. Introduction

In recent years the composite sandwich structures, which consist of two thin but stiff composite laminated facesheets bonded to a lightweight and thick core with low in-plane modulus, are widely used in transportations, marine, aeronautics and astronautics owing to the low weight and high rigidity. Similar to the flanged beam, in the sandwich structures the most of the in-plane membrane and bending forces are carried by the facesheets while the shear loads are transferred by the core. The complexity of the overall and local behavior of the sandwich structures has aroused a large number of computational methods.

The investigations of the computational models for incompressible sandwich structures started from Reissner [1] and many others [2–5]. One of the well-known conventional modeling approaches is the splitting rigidity approach [3–5]. Recently, the modeling scheme of composite sandwich structures is regarded as following the same analysis schemes of the composite laminated structures, such as the equivalent single layer theory (classical laminate theory and shear deformation laminated plate theories) [6–12], three-dimensional elastic theory (traditional 3-D elastic formulations, layerwise theory, unified formulation and generalized unified formulation) [13–17] and multiple model methods [18,19]. However, the response of composite sandwich structures is significantly affected by transverse shear deformation resulted from the large core thickness and wide variety in material properties along the thickness direction of the composite laminated facesheets. These influences cannot be considered adequately by the equivalent single layer theories. Consequently, the analysis of composite sandwich structures may require the layerwise or 3D elastic theory. Since the number of the exact 3D elasticity solutions is limited [20] and the 3D finite element analysis may need enormous computational cost, the layerwise theory would be a better choice compared to the equivalent single layer theory and 3D elasticity theory.

Hu [21] assessed the accuracy of the computational models based on various shear deformation theories and Zig–Zag theories in predicting the bending behavior of sandwich plates under static loading and the dynamic problem. It comes out from this assessment process that the Zig–Zag models are more accurate than the classical laminate theory and shear deformation theories. Ferreira [22,23] has studied the static deformations and free vibration problem with the layerwise theory and radial basis functions for laminated and sandwich plates. Roque [24] developed a trigonometric layerwise deformation theory for modeling symmetric composite plates and sandwich plates. Theofanis [25] presented a high-order discrete-layer theory for predicting the damping of composite laminated sandwich beams, in which the quadratic and cubic terms were involved when approximating the in-plane displacement in each discrete layer and the interlaminar shear stress continuity was imposed through the thickness. In addition, for the composite sandwich structures there are many other literatures studying the computational modeling by using the layerwise theories [26–29].

* Corresponding author. Tel.: +86 1062782078.
E-mail address: xzhang@tsinghua.edu.cn (X. Zhang).

1359-8368/$ - see front matter © 2013 Elsevier Ltd. All rights reserved.
http://dx.doi.org/10.1016/j.compositesb.2013.04.031

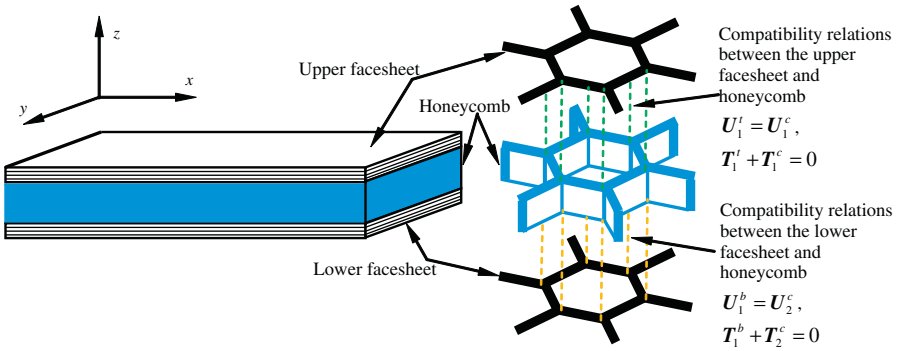

Fig. 1. Schematic diagram of the LW/SE method for the composite sandwich structures.

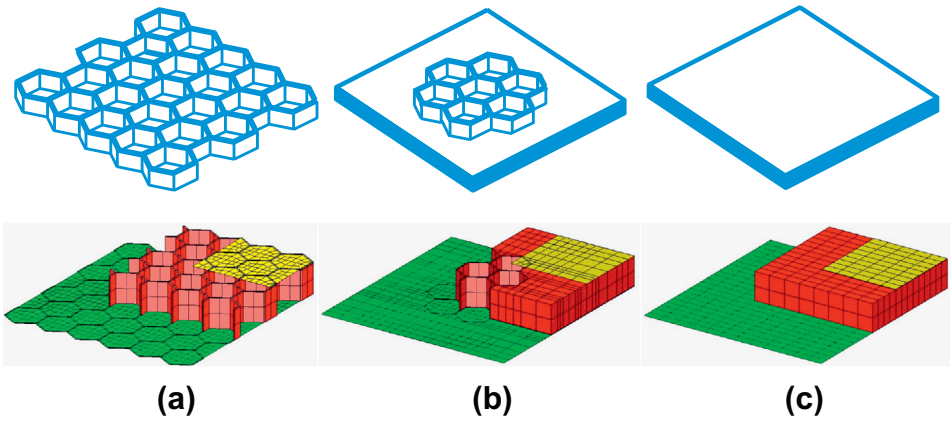

Fig. 2. Schematics diagram and meshing of three different modeling strategies for the honeycomb. (a) Full model, (b) local model, and (c) equivalent model.

The main emphasis of the above methods was to determine the overall global response. The use of a flexible core in modern sandwich structures subjected to partially distributed loads, point load and point supports yields localized deformations along the panel, in the form of indents, which are associated with inconsistent displacements of upper and lower facesheets. The detailed local damages morphology and failure process are very important for the impact dynamics analysis of the modern sandwich structures. Further, there are two more reasons which will lead to low accuracy of the above analysis schemes of the composite sandwich structures: one reason is that the material parameters calculated by the equivalent methods (such as sandwich theory [30]) cannot fully reflect the mechanical behavior of the core; another one is that the thick core reduces the analysis accuracy of the plates and shells theories which are usually employed to model the behavior of the facesheets and equivalent honeycomb. The core thickness of sandwich structures usually ranges between 3 and 26 mm [31]. Therefore, it is very necessary to develop an analysis scheme which not only can obtain the accurate local displacements and stresses of the facesheets and core but also can reduce the influence of the thickness and equivalent of core on the analysis accuracy at a reasonable computational cost.

The remarkable influence of the transverse shear deformation resulted from the high core thickness can be removed if the core is discretized independently by brick elements while the composite laminated facesheets are still simulated by the layerwise theory. Fortunately, unlike the equivalent single layer theories, the governing equations of facesheets established by the layerwise theory can be conveniently coupled with the governing equations of the core established by the brick elements based on the compatibility conditions at the interface between facesheets and core, since the degree of freedoms (DOFs) of the layerwise theory is equal to that of the brick element and the displacements variables of the upper and lower surface of facesheets appear in the governing equations. In this modeling scheme, if the overall or one part of the core is discretized by solid elements, the error introduced by the equivalent methods about the core properties [29] will disappear or decrease. In addition, the detailed local deformation of the facesheets and core can be obtained by using this scheme if the core cells belonging to the special attention area (key region) are modeled based on the real structure form completely instead of the equivalent form.

In present work, a layerwise/solid-element method is established, in which layerwise theory and the eight-noded solid elements are used to model the behaviors of the facesheets and the honeycomb, respectively. Based on the finite element formulation of the facesheets and the honeycomb, the governing equations of the composite sandwich plates are assembled by using the compatibility conditions at the interface. And the modeling method of the core is investigated in detail.

2. Layerwise laminate theory for composite laminated plates

In the layerwise laminate theory [18], the displacements at point (x, y, z) in the composite laminated plates are assumed to be

$$u(x,y,z) = \sum_{i=1}^{N+1} u_i(x,y)\phi^i(z),\ v(x,y,z) = \sum_{i=1}^{N+1} v_i(x,y)\phi^i(z),\ w(x,y,z) = \sum_{i=1}^{N+1} w_i(x,y)\phi^i(z) \quad (1)$$

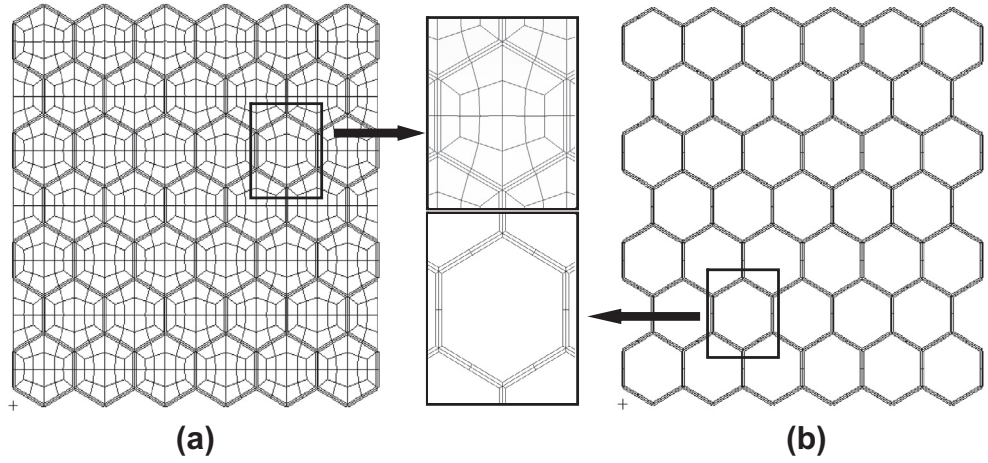

Fig. 3. Finite element mesh of the facesheets and the honeycomb of a sandwich structure. (a) Upper and lower facesheets and (b) honeycomb.

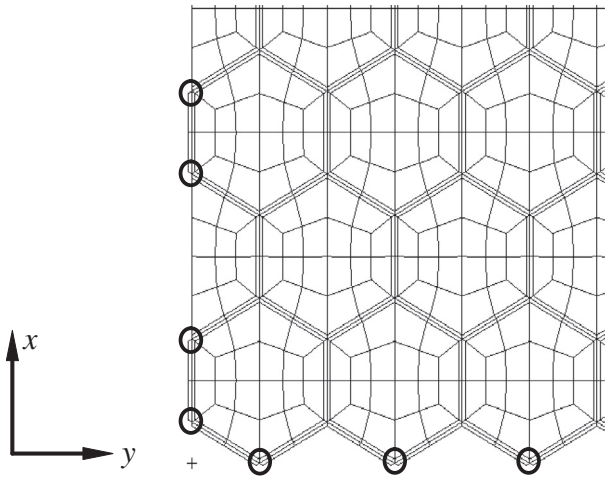

Fig. 4. The coordinate system and boundary conditions of the sandwich structure (one quarter model).

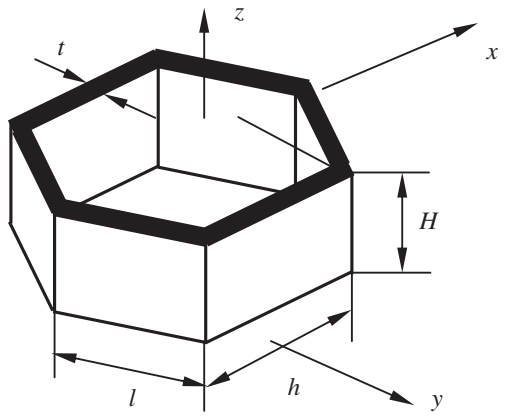

Fig. 5. Cell of honeycomb core.

where u, v and w represent the displacement components in the x, y and z directions, respectively. ϕ^i is a linear Lagrangian interpolation function through the thickness of the composite laminated plates. The transverse displacements are defined in terms of one-dimensional finite element approximation. The laminate thickness dimension is subdivided into a series of N one-dimensional finite elements ($N_e = N + 1$ nodes) whose nodes are located in planes parallel to xy plane in the undeformed laminate. u_i, v_i and w_i are the nodal values. N is also the number of mathematical layers of the laminated plates, which may be equal or less than the number of physical layers. For laminates containing plies of the same geometrical and material properties, it is often convenient to group these plies together to reduce the computational efforts.

In the small deformation problems, the strains associated with the displacement field Eq. (1) can be calculated as

$$\begin{aligned}
&\varepsilon_{xx}=\frac{\partial u}{\partial x}=\sum_{i=1}^{N+1}\frac{\partial u_i}{\partial x}\phi^i,\ \varepsilon_{yy}=\frac{\partial v}{\partial y}=\sum_{i=1}^{N+1}\frac{\partial v_i}{\partial y}\phi^i,\ \varepsilon_{zz}=\frac{\partial w}{\partial z}=\sum_{i=1}^{N+1}w_i\frac{d\phi^i}{dz},\\
&\gamma_{xz}=\frac{\partial u}{\partial z}+\frac{\partial w}{\partial x}=\sum_{i=1}^{N+1}u_i\frac{d\phi^i}{dz}+\sum_{i=1}^{N+1}\frac{\partial w_i}{\partial x}\phi^i,\ \gamma_{xy}=\frac{\partial u}{\partial y}+\frac{\partial v}{\partial x}=\sum_{i=1}^{N+1}\left(\frac{\partial u_i}{\partial y}+\frac{\partial v_i}{\partial x}\right)\phi^i,\\
&\gamma_{yz}=\frac{\partial v}{\partial z}+\frac{\partial w}{\partial y}=\sum_{i=1}^{N+1}v_i\frac{d\phi^i}{dz}+\sum_{i=1}^{N+1}\frac{\partial w_i}{\partial y}\phi^i,
\end{aligned}\tag{2}$$

The 3-D constitutive equations of an arbitrarily oriented orthotropic laminate in the laminate coordinate system are

$$\boldsymbol{\sigma}=\boldsymbol{C}\cdot\boldsymbol{\varepsilon}\tag{3}$$

where $\boldsymbol{\sigma}=[\sigma_{xx}\ \sigma_{yy}\ \sigma_{zz}\ \sigma_{yz}\ \sigma_{xz}\ \sigma_{xy}]$; $\boldsymbol{\varepsilon}=[\varepsilon_{xx}\ \varepsilon_{yy}\ \varepsilon_{zz}\ \gamma_{yz}\ \gamma_{xz}\ \gamma_{xy}]$; $C_{ij}(i,j=1,2,\ldots,6)$ denotes the elasticity coefficient of material.

In order to develop the finite element formulation, the displacement functions v_i and w_i are approximated on the i-th plane of the plate by

$$u_i=\sum_{n=1}^{n_{en}}u_i^n\varphi^n(x,y),\ v_i=\sum_{n=1}^{n_{en}}v_i^n\varphi^n(x,y),\ w_i=\sum_{n=1}^{n_{en}}w_i^n\varphi^n(x,y)\tag{4}$$

where n_{en} is the number of nodes in each element, $\varphi(x,y)$ is finite element shape function, u_i^n, v_i^n and w_i^n are the displacement components of n-th node of the 2D finite element representing the i-th plane of the physical laminates element.

The finite element formulation of the present layerwise theory can be derived using the principle of virtual displacements in matrix form as

$$\begin{bmatrix}{}^{11}\boldsymbol{M}_{ij}^{\alpha\beta} & \boldsymbol{0} & \boldsymbol{0}\\ \boldsymbol{0} & {}^{22}\boldsymbol{M}_{ij}^{\alpha\beta} & \boldsymbol{0}\\ \boldsymbol{0} & \boldsymbol{0} & {}^{33}\boldsymbol{M}_{ij}^{\alpha\beta}\end{bmatrix}\begin{Bmatrix}\ddot{\boldsymbol{u}}\\ \ddot{\boldsymbol{v}}\\ \ddot{\boldsymbol{w}}\end{Bmatrix}+\begin{bmatrix}{}^{11}\boldsymbol{K}_{ij}^{\alpha\beta} & {}^{12}\boldsymbol{K}_{ij}^{\alpha\beta} & {}^{13}\boldsymbol{K}_{ij}^{\alpha\beta}\\ {}^{21}\boldsymbol{K}_{ij}^{\alpha\beta} & {}^{22}\boldsymbol{K}_{ij}^{\alpha\beta} & {}^{23}\boldsymbol{K}_{ij}^{\alpha\beta}\\ {}^{31}\boldsymbol{K}_{ij}^{\alpha\beta} & {}^{32}\boldsymbol{K}_{ij}^{\alpha\beta} & {}^{33}\boldsymbol{K}_{ij}^{\alpha\beta}\end{bmatrix}\begin{Bmatrix}\boldsymbol{u}\\ \boldsymbol{v}\\ \boldsymbol{w}\end{Bmatrix}=\begin{Bmatrix}\boldsymbol{q}_u\\ \boldsymbol{q}_v\\ \boldsymbol{q}_w\end{Bmatrix}\tag{5}$$

where $i, j = 1,2,\ldots, n_{en}$. $\alpha, \beta = 1, 2,\ldots, N+1$, $\{\boldsymbol{u}, \boldsymbol{v}, \boldsymbol{w}\}^T$ denotes the interface displacements vectors, and $\{\boldsymbol{q}_u, \boldsymbol{q}_v, \boldsymbol{q}_w\}^T$ denotes the corre-

Table 1
Comparison of the maximum displacement w between the layerwise/solid-element and the 3D elastic method.

	N_c	Layerwise/solid-element method			3D elastic method		
		$N_s = 1$	$N_s = 2$	$N_s = 3$	$N_s = 4$	$N_s = 1$	$N_s = 2$
Lower surface	2	3.256×10^{-5}	3.295×10^{-5}	3.304×10^{-5}	3.304×10^{-5}	3.523×10^{-5}	3.545×10^{-5}
	3	3.056×10^{-5}	3.081×10^{-5}	3.085×10^{-5}	3.088×10^{-5}	3.124×10^{-5}	3.165×10^{-5}
Honeycomb	2	3.792×10^{-5}	3.837×10^{-5}	3.849×10^{-5}	3.854×10^{-5}	4.076×10^{-5}	4.092×10^{-5}
	3	3.765×10^{-5}	3.810×10^{-5}	3.822×10^{-5}	3.830×10^{-5}	4.012×10^{-5}	4.034×10^{-5}
Upper surface	2	8.763×10^{-5}	9.004×10^{-5}	9.098×10^{-5}	9.137×10^{-5}	1.123×10^{-4}	1.137×10^{-4}
	3	8.764×10^{-5}	9.000×10^{-5}	9.093×10^{-5}	9.134×10^{-5}	1.082×10^{-4}	1.103×10^{-4}

Table 2
Comparison of the natural frequencies between the layerwise/solid-element and the 3D elastic method.

Mode number	Layerwise/solid-element method						3D elastic method	
	$N_c = 2$			$N_c = 3$			$N_c = 2$	$N_c = 3$
	$N_s = 1$	$N_s = 2$	$N_s = 3$	$N_s = 1$	$N_s = 2$	$N_s = 3$	$N_s = 1$	$N_s = 2$
1	601.79	599.14	598.43	605.51	602.84	602.18	589.62	592.19
2	987.84	981.90	980.64	995.32	989.15	987.68	958.33	963.94
3	1027.1	1020.6	1019.1	1034.5	1027.8	1026.2	999.16	1005.0
4	1316.5	1306.5	1304.2	1326.4	1316.2	1313.7	1268.6	1277.6
5	1469.0	1457.0	1454.3	1480.6	1468.3	1465.4	1398.7	1409.8
6	1536.7	1523.0	1519.8	1547.7	1533.9	1530.7	1472.3	1483.6
7	1711.6	1702.6	1698.9	1702.8	1700.9	1700.2	1627.7	1642.4
8	1718.9	1709.1	1708.2	1732.0	1715.5	1711.6	1666.0	1680.6

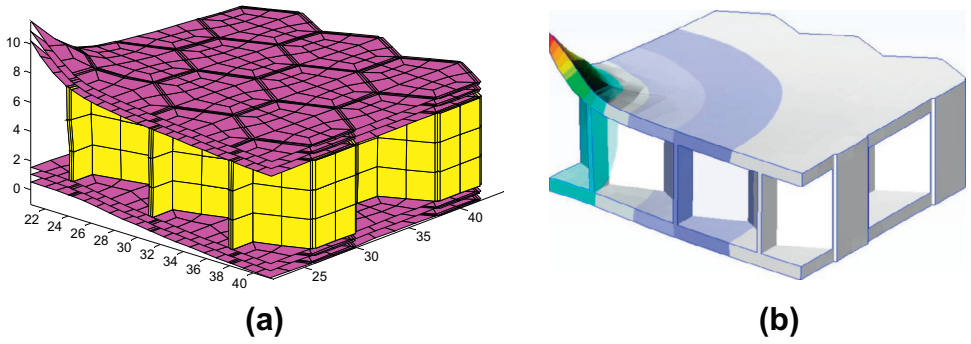

Fig. 6. Deformation of the sandwich structure obtained by. (a) Present layerwise/solid-element method and (b) 3D elastic method.

Table 3
Material properties of the facesheets and honeycomb.

Facesheets	$E_{XX} = 156500$ MPa, $E_{YY} = E_{ZZ} = 13{,}000$ MPa, $G_{YZ} = 4540$ MPa, $G_{XY} = G_{XZ} = 6960$ MPa, $\upsilon_{YZ} = 0.4$, $\upsilon_{XY} = \upsilon_{XZ} = 0.23$, $\rho = 2700$ kg/m^3
Honeycomb	$E = 68{,}000$ MPa, $\upsilon = 0.3$, $\rho = 2700$ kg/m^3
Equivalent properties of the honeycomb [30]	$E_{XX} = E_{YY} = 101.5758$ MPa, $E_{ZZ} = 5888.8$ MPa, $G_{YZ} = G_{XZ} = 1307.7$ MPa, $G_{XY} = 25.4978$ MPa, $\upsilon_{YZ} = 0.0$, $\upsilon_{XY} = 1.0$, $\upsilon_{ZX} = 0.3$, $\rho = 360$ kg/m^3

sponding load vectors that consist of boundary and force contributions. Stiffness matrix ${}^{mn}\boldsymbol{M}_{ij}^{\alpha\beta}$ can be found in Refs. [13,14].

3. Layerwise/solid-element method for composite laminated sandwich structures

The schematic diagram of the LW/SE method for the composite sandwich structures is shown in Fig. 1, where the upper and lower facesheets are discretized with the four-noded quadrilateral elements and the layerwise theory, while the core is discretized with the eight-noded solid elements. Based on the finite element formulations of the facesheets and core, the final governing equation of the composite sandwich structures can be assembled by using the compatibility conditions to ensure the continuity of displacements at the interface between facesheets and core. In the present work, the honeycomb is investigated, but other forms of core can also be solved in a similar way.

All of the displacements variables of the upper and lower facesheets can be divided into two groups: interface and internal displacements vector. The finite element model Eq. (5) of the

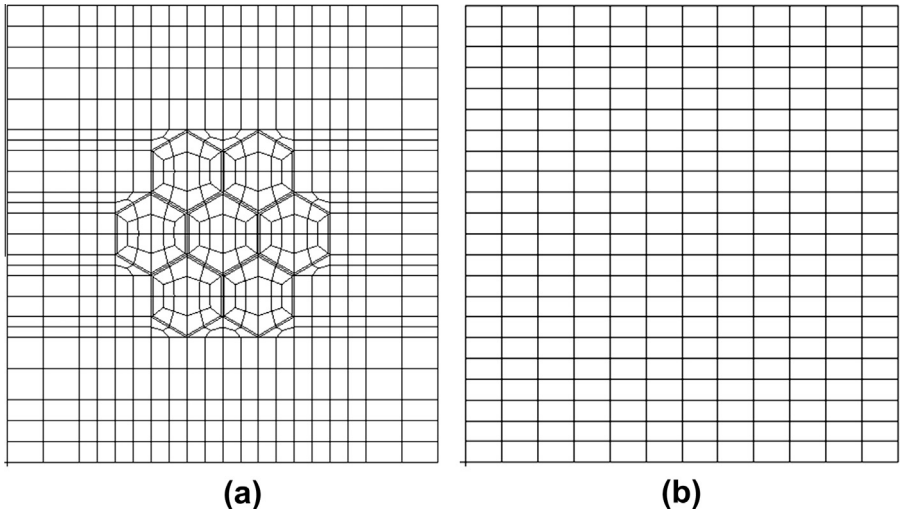

Fig. 7. Finite element discretization of the sandwich structure. (a) Local model and (b) equivalent model.

Table 4
The DOFs of the LW/SE method based on the full model, the local model and the equivalent model.

	Full model	Local model	Equivalent model
Facesheets	35,544	15,576	7176
Honeycomb	7578	4896	2691
Total	43,122	20,472	9867

laminated composite plates can be rewritten for the upper and lower facesheets as follows

$$\begin{bmatrix} \boldsymbol{M}_{11}^{t} & \boldsymbol{M}_{12}^{t} \\ \boldsymbol{M}_{21}^{t} & \boldsymbol{M}_{22}^{t} \end{bmatrix} \begin{Bmatrix} \ddot{\boldsymbol{U}}_{1}^{t} \\ \ddot{\boldsymbol{U}}_{2}^{t} \end{Bmatrix} + \begin{bmatrix} \boldsymbol{K}_{11}^{t} & \boldsymbol{K}_{12}^{t} \\ \boldsymbol{K}_{21}^{t} & \boldsymbol{K}_{22}^{t} \end{bmatrix} \begin{Bmatrix} \boldsymbol{U}_{1}^{t} \\ \boldsymbol{U}_{2}^{t} \end{Bmatrix} = \begin{Bmatrix} \boldsymbol{0} \\ \boldsymbol{F}_{2}^{t} \end{Bmatrix} + \begin{Bmatrix} \boldsymbol{T}_{1}^{t} \\ \boldsymbol{0} \end{Bmatrix} \tag{6a}$$

$$\begin{bmatrix} \boldsymbol{M}_{11}^{b} & \boldsymbol{M}_{12}^{b} \\ \boldsymbol{M}_{21}^{b} & \boldsymbol{M}_{22}^{b} \end{bmatrix} \begin{Bmatrix} \ddot{\boldsymbol{U}}_{1}^{b} \\ \ddot{\boldsymbol{U}}_{2}^{b} \end{Bmatrix} + \begin{bmatrix} \boldsymbol{K}_{11}^{b} & \boldsymbol{K}_{12}^{b} \\ \boldsymbol{K}_{21}^{b} & \boldsymbol{K}_{22}^{b} \end{bmatrix} \begin{Bmatrix} \boldsymbol{U}_{1}^{b} \\ \boldsymbol{U}_{2}^{b} \end{Bmatrix} = \begin{Bmatrix} \boldsymbol{0} \\ \boldsymbol{F}_{2}^{b} \end{Bmatrix} + \begin{Bmatrix} \boldsymbol{T}_{1}^{b} \\ \boldsymbol{0} \end{Bmatrix} \tag{6b}$$

where the superscript t and b denote upper and lower facesheet, respectively. The subscripts 1 and 2 denote the interface displacements vector and internal displacements vector, respectively. $\boldsymbol{U}\ddot{\boldsymbol{U}}$,

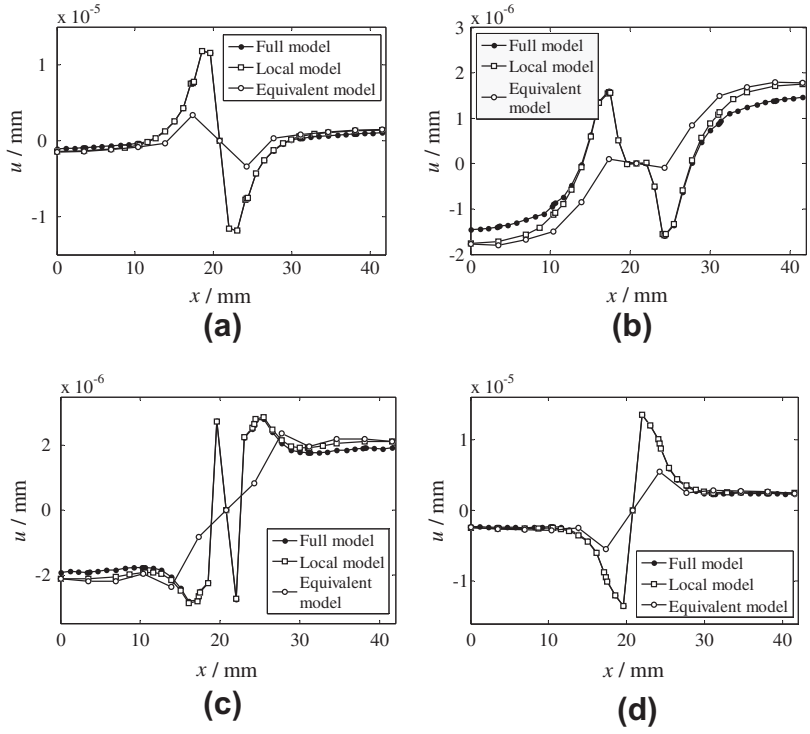

Fig. 8. In-plane distributions of the displacement u in the upper facesheet obtained by the LW/SE methods based on three different modeling schemes. (a) Lower surface, (b) interface between the first layer and second layer, (c) interface between the second layer and third layer, and (d) upper surface.

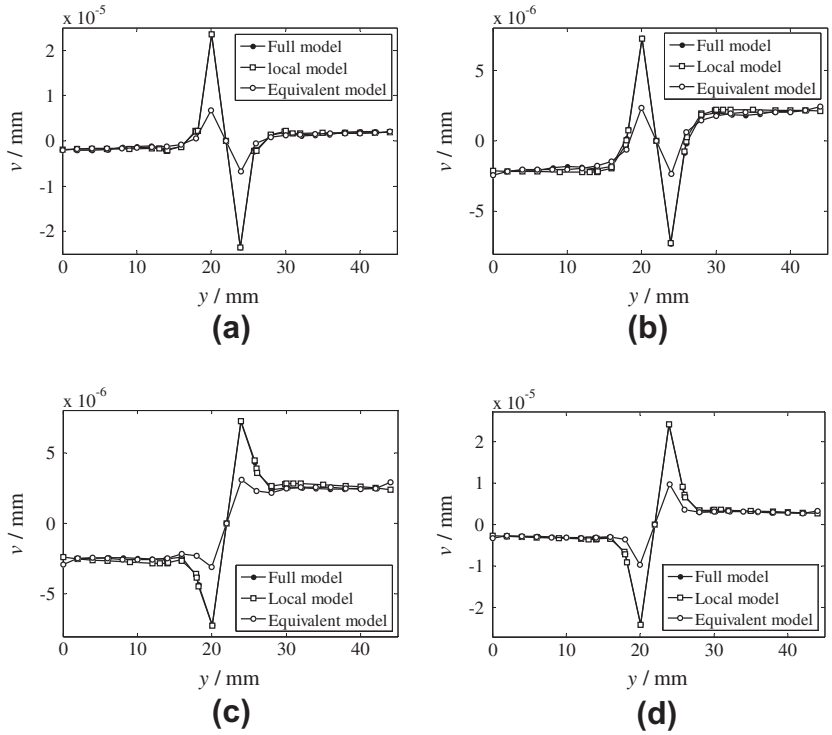

Fig. 9. In-plane distributions of the displacement v in the upper facesheet obtained by the LW/SE methods based on three different modeling schemes. (a) Lower surface, (b) interface between the first layer and second layer, (c) interface between the second layer and third layer, and (d) upper surface.

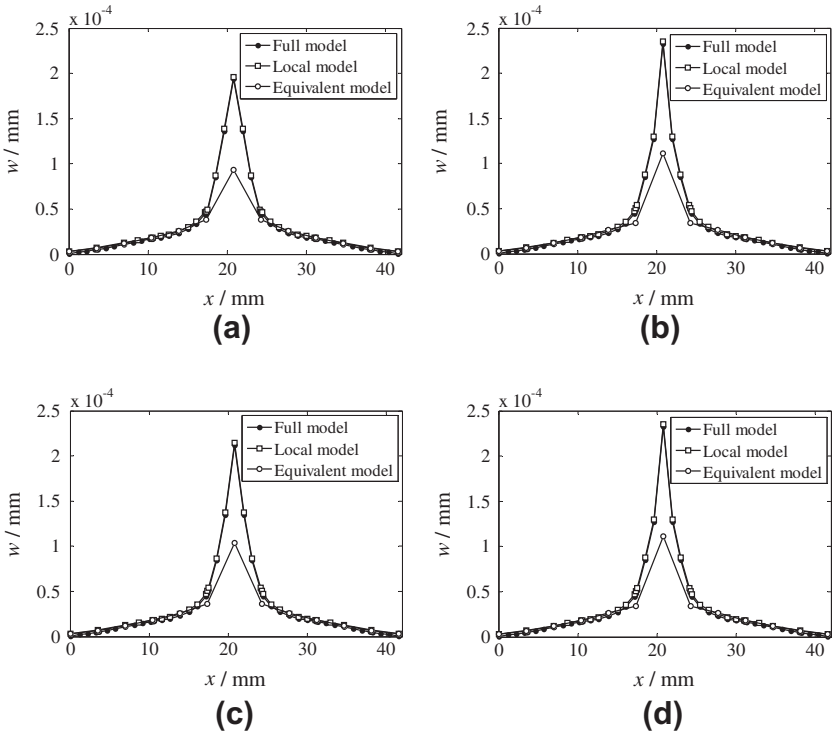

Fig. 10. In-plane distributions of the displacement w in the upper facesheet obtained by the LW/SE methods based on three different modeling schemes. (a) Lower surface, (b) interface between the first layer and second layer, (c) interface between the second layer and third layer, and (d) upper surface.

$\boldsymbol{F}$ and $\boldsymbol{T}$ are the displacements, accelerations, external loads vector and interaction force between the facesheets and core, respectively.

Similarly, all of the displacements variables of the honeycomb can also be divided into three groups so that the finite element formulation of the core can be expressed as

$$\begin{bmatrix} \boldsymbol{M}^c_{11} & \boldsymbol{M}^c_{12} & \boldsymbol{M}^c_{13} \\ \boldsymbol{M}^c_{21} & \boldsymbol{M}^c_{22} & \boldsymbol{M}^c_{23} \\ \boldsymbol{M}^c_{31} & \boldsymbol{M}^c_{32} & \boldsymbol{M}^c_{33} \end{bmatrix} \begin{Bmatrix} \ddot{\boldsymbol{U}}^c_{1,t} \\ \ddot{\boldsymbol{U}}^c_{1,b} \\ \ddot{\boldsymbol{U}}^c_{2} \end{Bmatrix} + \begin{bmatrix} \boldsymbol{K}^c_{11} & \boldsymbol{K}^c_{12} & \boldsymbol{K}^c_{13} \\ \boldsymbol{K}^c_{21} & \boldsymbol{K}^c_{22} & \boldsymbol{K}^c_{23} \\ \boldsymbol{K}^c_{31} & \boldsymbol{K}^c_{32} & \boldsymbol{K}^c_{33} \end{bmatrix} \begin{Bmatrix} \boldsymbol{U}^c_{1,t} \\ \boldsymbol{U}^c_{1,b} \\ \boldsymbol{U}^c_{2} \end{Bmatrix} = \begin{Bmatrix} \boldsymbol{0} \\ \boldsymbol{0} \\ \boldsymbol{F}^c_{2} \end{Bmatrix} + \begin{Bmatrix} \boldsymbol{T}^c_{1,t} \\ \boldsymbol{T}^c_{1,b} \\ \boldsymbol{0} \end{Bmatrix} \tag{7}$$

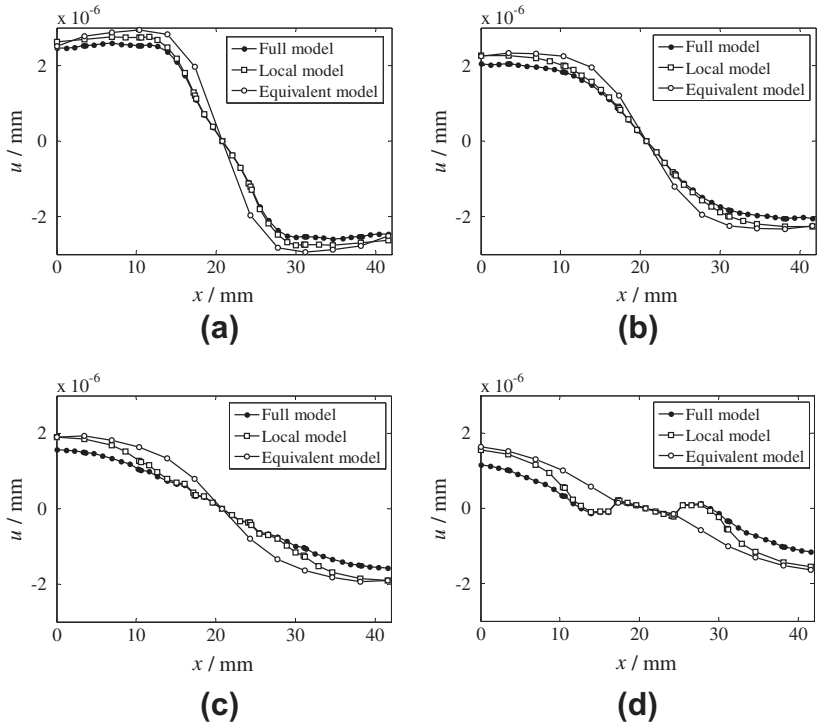

Fig. 11. In-plane distributions of the displacement u in the lower facesheet obtained by the LW/SE methods based on three different modeling schemes. (a) Lower surface, (b) interface between the first layer and second layer, (c) interface between the second layer and third layer, and (d) upper surface.

where the superscript c denotes honeycomb of the sandwich structures. $\boldsymbol{U}^c_{1,t}$ and $\boldsymbol{U}^c_{1,b}$ are the interface displacement vectors of the honeycomb at the upper facesheet and the lower facesheet, respectively, and $\boldsymbol{U}^c_2$ is the internal displacements vector.

According to the compatibility relations between the upper facesheet and core ($\boldsymbol{U}^t_1 = \boldsymbol{U}^c_{1,t}$ and $\boldsymbol{T}^t_1 + \boldsymbol{T}^c_{1,t} = 0$), the summation of the first row of Eqs. (6a) and (7) yields

$$(\boldsymbol{K}^t_{11} + \boldsymbol{K}^c_{11})\boldsymbol{U}^t_1 + \boldsymbol{K}^t_{12}\boldsymbol{U}^t_2 + \boldsymbol{K}^c_{12}\boldsymbol{U}^c_{1,b} + \boldsymbol{K}^c_{13}\boldsymbol{U}^c_2 + \left[(\boldsymbol{M}^t_{11} + \boldsymbol{M}^c_{11})\ddot{\boldsymbol{U}}^t_1 + \boldsymbol{M}^t_{12}\ddot{\boldsymbol{U}}^t_2 + \boldsymbol{M}^c_{12}\ddot{\boldsymbol{U}}^c_{1,b} + \boldsymbol{M}^c_{13}\ddot{\boldsymbol{U}}^c_2\right] = \boldsymbol{0} \tag{8a}$$

According to the compatibility relations between the lower facesheet and core ($\boldsymbol{U}^b_1 = \boldsymbol{U}^c_{1,b}\boldsymbol{T}^b_1 + \boldsymbol{T}^c_{1,b} = 0$), similarly we have

$$\boldsymbol{K}^c_{21}\boldsymbol{U}^t_1 + (\boldsymbol{K}^b_{11} + \boldsymbol{K}^c_{22})\boldsymbol{U}^b_1 + \boldsymbol{K}^b_{12}\boldsymbol{U}^b_2 + \boldsymbol{K}^c_{23}\boldsymbol{U}^c_2 + \left[\boldsymbol{M}^c_{21}\ddot{\boldsymbol{U}}^t_1 + (\boldsymbol{M}^b_{11} + \boldsymbol{K}^c_{22})\ddot{\boldsymbol{U}}^b_1 + \boldsymbol{M}^b_{12}\ddot{\boldsymbol{U}}^b_2 + \boldsymbol{M}^c_{23}\ddot{\boldsymbol{U}}^c_2\right] = \boldsymbol{0} \tag{8b}$$

The final discrete equations of the composite sandwich structures can be obtained by combining Eqs. (8a) and (8b), the second row of Eqs. (6a) and (6b), and the third row of Eq. (7) as

$$\begin{bmatrix} \boldsymbol{M}^t_{11}+\boldsymbol{M}^c_{11} & \boldsymbol{M}^t_{12} & \boldsymbol{M}^c_{12} & \boldsymbol{0} & \boldsymbol{M}^c_{13} \\ \boldsymbol{M}^t_{21} & \boldsymbol{M}^t_{22} & \boldsymbol{0} & \boldsymbol{0} & \boldsymbol{0} \\ \boldsymbol{M}^c_{21} & \boldsymbol{0} & \boldsymbol{M}^b_{11}+\boldsymbol{M}^c_{22} & \boldsymbol{M}^b_{12} & \boldsymbol{M}^c_{23} \\ \boldsymbol{0} & \boldsymbol{0} & \boldsymbol{M}^b_{21} & \boldsymbol{M}^b_{22} & \boldsymbol{0} \\ \boldsymbol{M}^c_{31} & \boldsymbol{0} & \boldsymbol{M}^c_{32} & \boldsymbol{0} & \boldsymbol{M}^c_{33} \end{bmatrix} \begin{Bmatrix} \ddot{\boldsymbol{U}}^t_1 \\ \ddot{\boldsymbol{U}}^t_2 \\ \ddot{\boldsymbol{U}}^b_1 \\ \ddot{\boldsymbol{U}}^b_2 \\ \ddot{\boldsymbol{U}}^c_2 \end{Bmatrix} + \begin{bmatrix} \boldsymbol{K}^t_{11}+\boldsymbol{K}^c_{11} & \boldsymbol{K}^t_{12} & \boldsymbol{K}^c_{12} & \boldsymbol{0} & \boldsymbol{K}^c_{13} \\ \boldsymbol{K}^t_{21} & \boldsymbol{K}^t_{22} & \boldsymbol{0} & \boldsymbol{0} & \boldsymbol{0} \\ \boldsymbol{K}^c_{21} & \boldsymbol{0} & \boldsymbol{K}^b_{11}+\boldsymbol{K}^c_{22} & \boldsymbol{K}^b_{12} & \boldsymbol{K}^c_{23} \\ \boldsymbol{0} & \boldsymbol{0} & \boldsymbol{K}^b_{21} & \boldsymbol{K}^b_{22} & \boldsymbol{0} \\ \boldsymbol{K}^c_{31} & \boldsymbol{0} & \boldsymbol{K}^c_{32} & \boldsymbol{0} & \boldsymbol{K}^c_{33} \end{bmatrix} \begin{Bmatrix} \boldsymbol{U}^t_1 \\ \boldsymbol{U}^t_2 \\ \boldsymbol{U}^b_1 \\ \boldsymbol{U}^b_2 \\ \boldsymbol{U}^c_2 \end{Bmatrix} = \begin{Bmatrix} \boldsymbol{0} \\ \boldsymbol{F}^t_2 \\ \boldsymbol{0} \\ \boldsymbol{F}^b_2 \\ \boldsymbol{F}^c_2 \end{Bmatrix} \tag{9}$$

If all details of the honeycomb structures are discretized (see Fig. 2a, referred as full model), it will result in unacceptable computational cost since the element size is determined by the characteristic length of the honeycomb cells which is much smaller than that of the sandwich structures. In order to remedy this limitation, the honeycomb can be firstly integrally considered as the anisotropic material by using some equivalent theories (such as sandwich plate theory [30]) and then discretized by brick elements in equivalent model as shown in Fig. 2c. Although the equivalent model greatly reduces the computational cost and the difficulty of the algorithm, at the same time, compared to the full model it reduces the analysis accuracy and cannot obtain the detailed local deformation which is resulted from the point load and point supports.

The local model illustrated in Fig. 2b, in which the honeycomb cells in the key region are modeled based on the real microstructure form completely instead of the equivalent anisotropic materials, is a combination of the full model and equivalent model. The local model possesses the advantages of the full model and equivalent model. The LW/SE method based on the local model reduces the computational cost compared to the full model and at the same time ensures the accuracy of the key area compared to the equivalent model.

4. Numerical examples

The meshing of the facesheets and honeycomb is carried out by MSC.Patran.

4.1. Validation of the present layerwise/solid-element method

The accuracy of the LW/SE method is validated by studying the honeycomb of a rectangular sandwich plate which consists of six regular hexagons honeycomb cells in x-direction and seven regular hexagons honeycomb cells in y-direction. The finite element discretization of the facesheets and honeycomb is shown in Fig. 3, where the discretization of the upper and lower facesheets should be consistent with that of the honeycomb in the interface. The sandwich plate with four clamped edges is subjected to a central

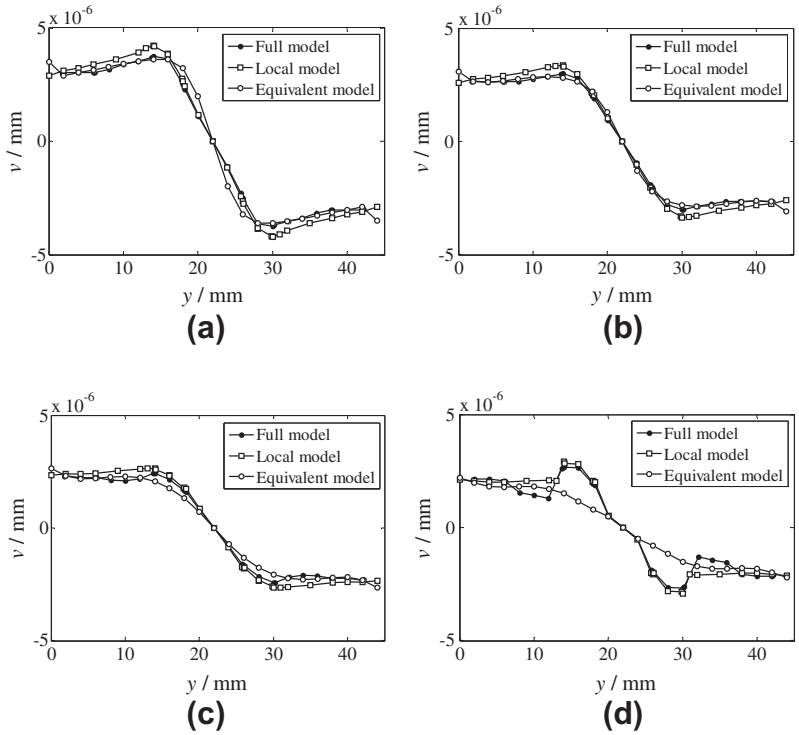

Fig. 12. In-plane distributions of the displacement v in the lower facesheet obtained by the LW/SE methods based on three different modeling schemes. (a) Lower surface, (b) interface between the first layer and second layer, (c) interface between the second layer and third layer, and (d) upper surface.

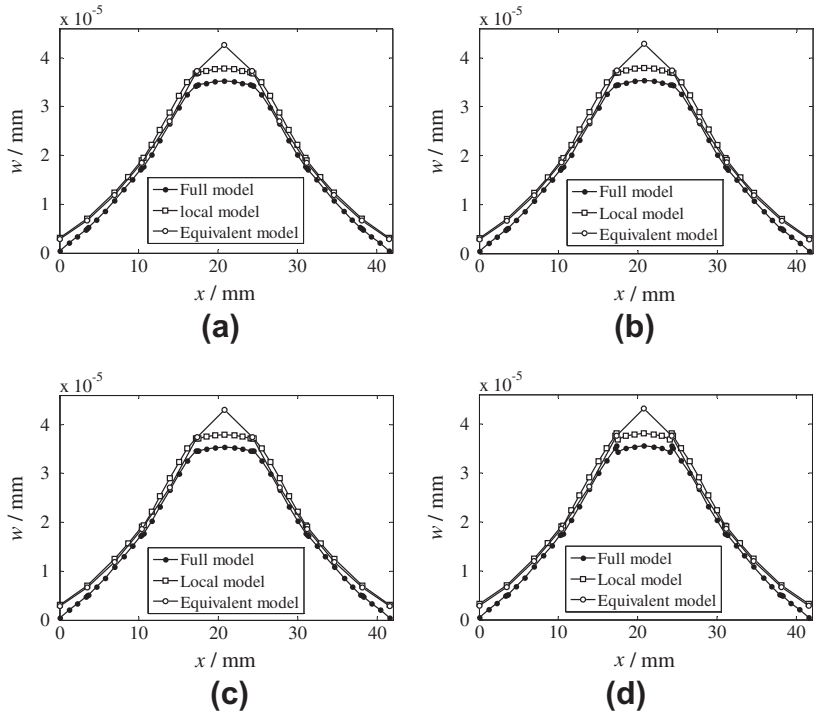

Fig. 13. In-plane distributions of the displacement w in the lower facesheet obtained by the LW/SE methods based on three different modeling schemes. (a) Lower surface, (b) interface between the first layer and second layer, (c) interface between the second layer and third layer, and (d) upper surface.

point load of the magnitude $F = 1$ N on the upper facesheet. The coordinate system and the boundary conditions are shown in Fig. 4. The sizes of regular hexagons honeycomb cells are $l = h = 4$ mm, $H = 6$ mm, and $t = 0.3464$ mm. The schematic diagram of the cell of the honeycomb is shown in Fig. 5. Material properties are taken as $E = 68{,}000$ MPa, $\upsilon = 0.3$ and $\rho = 2700$ kg/m^3. The facesheets and honeycomb have the same material properties.

For comparison purpose, a 3-D finite element analysis model is constructed using MSC.Patran and solved by MSC.Nastran, in which both of the facesheets and the honeycomb are discretized

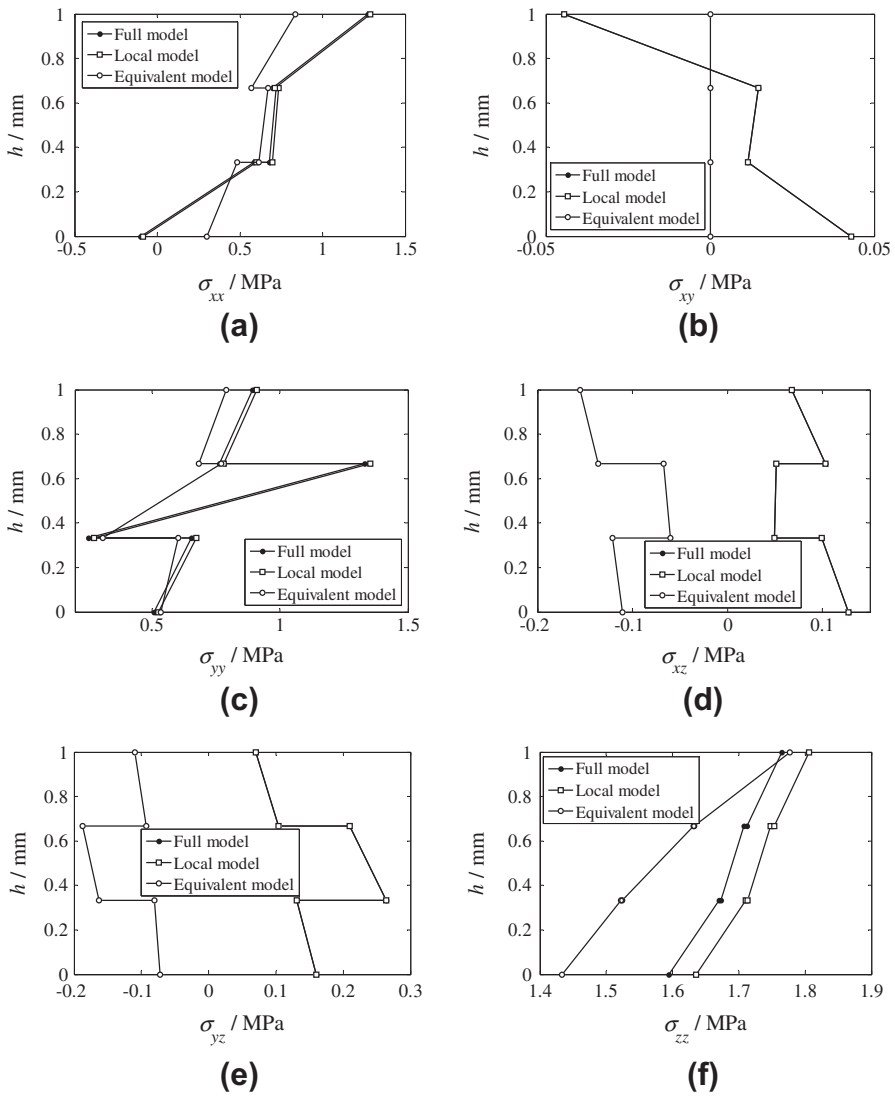

Fig. 14. Stresses of the upper facesheet of the sandwich structure obtained by the LW/SE methods based on three different modeling schemes. (a) σ_{xx}, (b) σ_{xy}, (c) σ_{yy}, (d) σ_{xz}, (e) σ_{yz} and (f) σ_{zz}.

by 8-node Hex Solid64 elements. The LW/SE method and the 3D elastic analysis model have the same meshing in the *xy* plane.

The maximum displacement *w* and the natural frequencies obtained by LW/SE method and 3D elastic method are compared in Tables 1 and 2, respectively, where N_s and N_c are the mathematic layer number of the facesheets and the element number of the honeycomb along the thickness direction respectively. The deformation of the sandwich structure obtained by the two methods with $N_c = 3$ and $N_s = 2$ is shown in Fig. 6. It can be seen from Tables 1 and 2 that the values of the maximum displacement *w* and the natural frequencies obtained by the present LW/SE method are in good agreement with those obtained by the 3D elastic method. The mathematic layer number of honeycomb N_c has a more significant effect on the results than the mathematic layer number of facesheets N_s. An important reason may be that the thickness of the honeycomb is greater than that of the facesheets. Under the load conditions in this example, the displacements of the upper facesheet are much larger than those of the lower facesheet, which means that the area around concentrated load would appear evident localized deformation in the form of indent. In the LW/SE method, because the details of the honeycomb structures are discretized by the solid elements instead of the equivalent anisotropic materials, the analysis accuracy for both the maximum displacement *w* and the natural frequencies is improved greatly compared to the traditional sandwich analysis methods.

4.2. Comparative analysis of the present three different equivalent schemes

The purpose of this example is to investigate the performance of the present three different modeling schemes shown in Fig. 2. The composite sandwich plate employed in this numerical example and that employed in Section 4.1 have the same geometry and boundary conditions. The stacking sequence of the upper and lower facesheets is [0/90/0]. All layers of the upper and lower facesheets have the same material properties. Material properties of the upper and lower facesheets, honeycomb, and the equivalent honeycomb are listed in Table 3.

The finite element discretization of the composite sandwich plate based on the full model is shown in Fig. 3. The finite element discretization of the composite sandwich plate based on the local model and the equivalent model are shown in Fig. 7, where the finite element discretization of the upper and lower facesheets is also consistent with that of the honeycomb in the contact area.

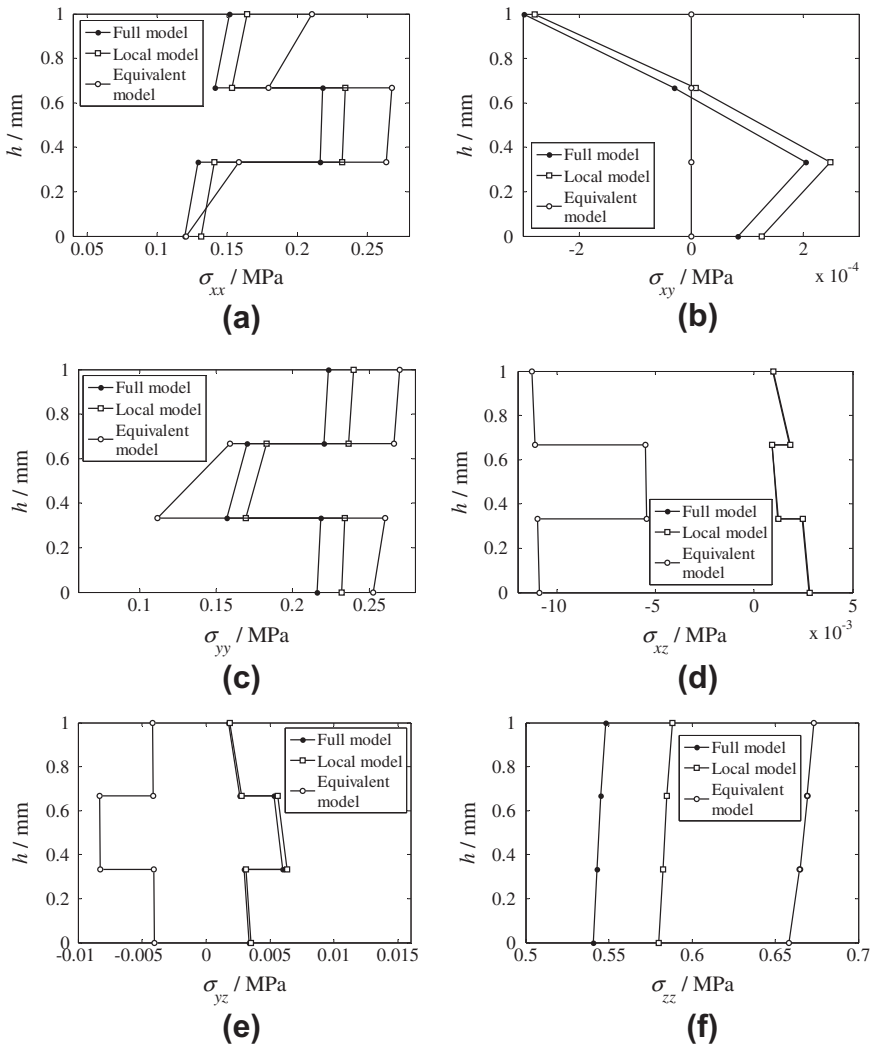

Fig. 15. Stresses of the lower facesheet of the sandwich plate obtained by the LW/SE methods based on three different modeling schemes. (a) σ_{xx}, (b) σ_{xy}, (c) σ_{yy}, (d) σ_{xz}, (e) σ_{yz} and (f) σ_{zz}.

The DOFs of the LW/SE models based on the full model, the local model and the equivalent model are listed in Table 4, where $N_s = 3$ and $N_c = 3$. The LW/SE method based on the equivalent model has lowest computational cost and difficulty of implementation. But the computational cost and difficulty of implementation of the LW/SE method based on the local model would close to that of equivalent model, if the size of the area of special attention is very small compared with the size of the whole sandwich plate.

Along the centerline in the x or y direction, the displacement distributions of the upper and lower facesheets of the composite sandwich plate obtained by three different modeling schemes are shown in Figs. 8–13 respectively, where the displacements u and w is distributed along the centerline in the x direction, while the displacement v is distributed along the centerline in y direction because the displacement v on the centerline in y direction equals zero. It can be seen from Figs. 8–13 that:

1. The displacements obtained by the local model and the equivalent model are in good agreement with those obtained by the full model.
2. The local model can provide accurate displacements in entire problem domains especially in the local area around the concentrated load and the surface of the facesheets. So the results of the local model are more reasonable than that of the equivalent model.
3. As a result of the behavior of the local model, the displacements obtained by the local model agree with those obtained by the full model in the area where the honeycomb cells are modeled based on the real structure form completely. However, in the area where the honeycomb cells are equivalent to anisotropic materials by using sandwich theory, the results of the local model are in good agreement with that of the equivalent model.
4. In the area where the honeycomb cells are equivalent to the anisotropic materials, for the local model and the equivalent model the displacements in the upper facesheet are closer to those of the full model than that in the lower facesheet. The point load is subjected on the upper facesheet and the direction is vertically upward, so the influence of the equivalent of the honeycomb on the analysis results of the upper facesheet is less than that of the lower facesheet.
5. In the area where the honeycomb cells are modeled based on the real structure form completely, the LW/SE method based on the equivalent model in the lower facesheet is more accurate than in the upper facesheet. One important reason is that local effect resulted from the point load is not significant in the lower facesheets (see Figs. 9–12).

Table 5
Nature frequencies of the sandwich structure obtained by the LW/SE methods.

	Mode number							
	1	2	3	4	5	6	7	8
Full model	544.4556	864.0444	952.3632	1163.199	1255.012	1337.558	1412.979	1467.307
Local model	500.2385	788.2661	863.6190	1069.856	1099.862	1150.257	1301.443	1346.923
Equivalent model	505.4335	807.5777	877.7303	1081.586	1177.806	1184.447	1326.649	1346.195

At the center points of the upper and lower facesheets, the thickness distributions of out-plane and in-plane stresses in the thickness direction obtained by three different modeling schemes are shown in Figs. 14 and 15. It is important to notice that the center points of the upper and lower facesheets belong to the interface where the honeycomb cells are modeled based on the real structure form completely. It can be seen from Figs. 14 and 15 that:

1. At the center point of the upper and lower facesheets, the stresses obtained by the local model are in good agreement with those obtained by the full model. Furthermore, the distribution curves of the shear stresses σ_{xy}, σ_{xz} and σ_{yz} in the upper facesheet and the shear stress σ_{xz} in the lower facesheet obtained by the local model coincide with those obtained by the full model.
2. For the equivalent model, but only the distribution of the normal stresses of the equivalent model agree with that obtained by the full model. Therefore, under the concentrate load the analysis schemes based on entire equivalent of honeycomb would be unable to provide reasonable stresses in the local area nearby the concentrate load.
3. Similar to the displacements, for the local model and the equivalent model (especially the local model), the stresses in the upper facesheet are closer to those of the full model than that in the lower facesheet.

The first 8 natural frequencies of the sandwich structure obtained by the LW/SE methods are listed in Table 5. It is obvious that the natural frequencies of the LW/SE methods based on the local model and the equivalent model are very close and differ slightly from the results of the full model. Compared to the full model, the errors of the local model and the equivalent model are resulted from the equivalent material properties of the honeycomb. Since the natural frequencies represent the overall characteristic of the sandwich structures, it stands to reason that the performance of the LW/SE methods based on the local model and the equivalent model are very close for the free vibration analysis.

5. Concluding remarks

A LW/SE method is established based on the layerwise laminate theory and 3D solid finite element method for the composite sandwich plates. And the modeling approach of the honeycomb is also investigated in detail.

For the problems of linear static and free vibration analysis the LW/SE method is reliable compared with the 3D elastic method. Furthermore, the LW/SE method can obtain accurate displacements and stresses in the static problem for the composite laminated facesheets with various forms of complex core. So the present analysis scheme can be further generalized for structures such as foam and truss core sandwich.

For the static problem under concentrate load, the LW/SE method based on the full model possesses the best accuracy but is the most time-consuming, while the LW/SE method based on the equivalent model provides the least computational cost and the worst accuracy especially in the area nearby the concentrate load. The LW/SE method based on local model has the balance between the accuracy and the computational burden. However, the performance of the LW/SE methods based on the local model and the equivalent are very close for the free vibration analysis.

Acknowledgements

This work was supported by the National Basic Research Program of China (2010CB832701) and the National Natural Science Foundation of China (11102097).

References

[1] Reissner E. Finite deflections of sandwich plates. J Aeronaut Sci 1948;15:435–40.
[2] Noor AK, Burton WS, Bert CW. Computational models for sandwich panels and shells. Appl Mech Rev 1996;49:155–99.
[3] Plantema FJ. Sandwich construction. New York: Wiley; 1966.
[4] Allen HG. Analysis and design of structural sandwich panels. Oxford: Pergamon Press; 1969.
[5] Zenkert D. An introduction to sandwich construction. London: Chameleon Press Ltd.; 1995.
[6] Yang HTY, Saigal S, Masud A, Kapania RK. A survey of recent shell finite elements. Int J Numer Meth Eng 2000;47:101–27.
[7] Reddy JN. A simple higher-order theory for laminated composite plates. J Appl Mech 1984;51:745–52.
[8] Reddy JN. A refined non-linear theory of plates with transverse shear deformation. Int J Solids Struct 1984;20:881–96.
[9] Reddy JN. A general non-linear third-order theory of plates with moderate thickness. Int J Non-Linear Mech 1990;25(6):677–86.
[10] Noor AK, Burton WS. Assessment of shear deformation theories for multilayered composite plates. Appl Mech Rev 1989;42(1):1–13.
[11] Whitney JM. The effect of transverse shear deformation in the bending of laminated plates. J Compos Mater 1969;3:534–47.
[12] Reissner E. Note on the effect of transverse shear deformation in laminated anisotropic plates. Comput Methods Appl Mech Eng 1979;20:203–9.
[13] Reddy JN. An evaluation of equivalent-single-layer and layerwise theories of composite laminates. Compos Struct 1993;25:21–35.
[14] Robbins DH, Reddy JN. Modeling of thick composites using a layer-wise laminated theory. Int J Numer Methods Eng 1993;36:655–77.
[15] Carrera E. Developments, ideas and evaluations based upon Reissner's mixed variational theorem in modeling of multilayered plates and shells. Appl Mech Rev 2001;54(4):301–29.
[16] Carrera E. Theories and finite elements for multilayered plates and shells: a unified compact formulation with numerical assessment and benchmarking. Arch Comput Methods Eng 2003;10(3):215–96.
[17] Luciano D. ∞^3 Hierarchy plate theories for thick and thin composite plates: the generalized unified formulation. Compos Struct 2008;84:256–70.
[18] Reddy JN. Mechanics of laminated composite plates and shells: theory and analysis. second ed. Washington, DC: CRC press; 2003.
[19] Reddy JN, Arciniega RA, Moleiro F. Finite element analysis of composite plates and shells. Encyclopedia of Aerospace Engineering; 2010.
[20] Noor AK, Burton WS. Stress and free vibration analysis of multilayered composite plates. Comput Struct 1989;11:183–204.
[21] Hu H, Belouettar S, Potier-Ferry M, Daya EM. Review and assessment of various theories for modeling sandwich composites. Compos Struct 2008;84:282–92.
[22] Ferreira AJM, Fasshauer GE, Batra RC, Rodrigues JD. Static deformations and vibration analysis of composite and sandwich plates using a layerwise theory and RBF-PS discretizations with optimal shape parameter. Compos Struct 2008;86:328–43.
[23] Ferreira AJM, Roque CMC, Jorge RMN, Kansa EJ. Static deformations and vibration analysis of composite and sandwich plates using a layerwise theory and multiquadrics discretizations. Eng Anal Bound Elem 2005;29:1104–14.
[24] Roque CMC, Ferreira AJM, Jorge RMN. Modelling of composite and sandwich plates by a trigonometric layerwise deformation theory and radial basis functions. Compos Part-B Eng 2005;36:559–72.
[25] Plagianakos Theofanis S, Saravanos Dimitris A. High-order layerwise mechanics and finite element for the damped dynamic characteristics of sandwich composite beams. Int J Solids Struct 2004;41:6853–71.

[26] Moreira RAS, Dias Rodrigues J. A layerwise model for thin soft core sandwich plates. Comput Struct 2006;84:1256–63.
[27] Mantari JL, Oktem AS, Guedes Soares C. A new trigonometric layerwise shear deformation theory for the finite element analysis of laminated composite and sandwich plates. Comput Struct 2012;94–95:45–53.
[28] Castro Luís MS, Ferreira AJM, Silvia Bertoluzza, Batra RC, Reddy JN. A wavelet collocation method for the static analysis of sandwich plates using a layerwise theory. Compos Struct 2010;92:1786–92.
[29] Ćetković M, Vuksanović DJ. Bending, free vibrations and buckling of laminated composite and sandwich plates using a layerwise displacement model. Compos Struct 2009;88:219–27.
[30] Gibson LJ, Ashby MF. Cellular solids structure and properties. second ed. University of Cambridge Press; 1999.
[31] Diamanti K, Soutis C, Hodgkinson JM. Non-destructive inspection of sandwich and repaired composite laminated structures. Compos Sci Technol 2005;65:2059–67.